Supporting Information

Low-temperature ohmic contacts to n-ZnSe for all-electrical quantum devices

Johanna Janßen,*,† Felix Hartz,‡ Till Huckemann,‡ Christian Kamphausen,‡ Malte Neul,‡ Lars R. Schreiber,‡ and Alexander Pawlis*,†

†*Peter Grünberg Institute 9 and JARA - FIT, Forschungszentrum Jülich GmbH, Germany*

‡*JARA - Institute for Quantum Information, RWTH Aachen University, Germany*

E-mail: jo.janssen@fz-juelich.de; a.pawlis@fz-juelich.de

Post implantation annealing

After ion implantation, an annealing step was conducted to recover the crystal structure, activate donors and thereby reduce the electrical resistance. Regarding the development of a fabrication technique to contact the 2-DEG in a ZnMgSe/ZnSe/ZnMgSe quantum well (QW) structure, the suitable temperature range of annealing is limited and can lead to degradation of the ZnSe/ZnMgSe interfaces by interdiffusion. Such degradation has been shown by photoluminescence investigations of similar QWs after rapid-thermal annealing for 30 s at about 400 °C.[1] Consequently, we focused our investigations on annealing temperatures around 250 °C to 300 °C according to typical MBE growth conditions of ZnSe. After application of an annealing step for 3 min at 250 °C a substantial improvement of the conductivity was achieved. However, a distinct increase of the resistance in the electrical measurements of the samples B* and C* is observed after a second 3 min long annealing step at 300 °C

was applied. Exemplary IV-characteristics of sample C* before (red) and after (green) the second annealing step are shown in Fig. S1.

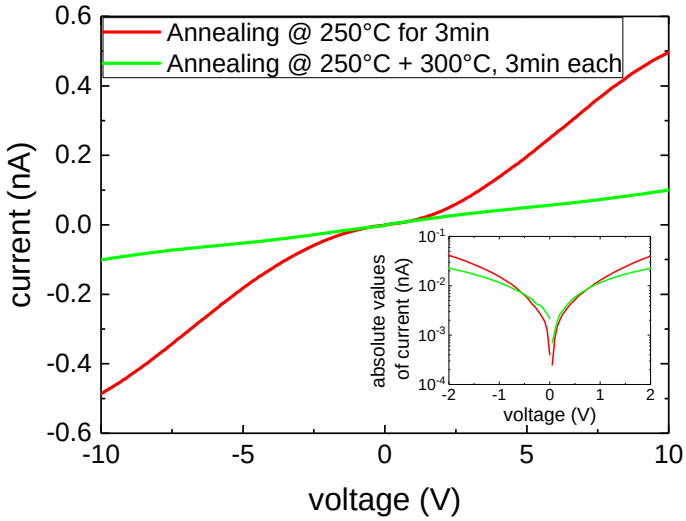

Figure S1: IV curves for sample C*obtained before and after the additional annealing step at 300 °C. The inset shows the logarithmic representation of the data.

Doping of ZnSe with Chlorine during MBE growth

A common doping technique for semiconductors is the doping during MBE growth. For doping of the ZnSe layer F and Cl were studied using a ZnF_2 and $ZnCl_2$ effusion cell, respectively, and the doping concentration was controlled by adjusting the cell temperature. In case of F, doping concentrations in the order of $10^{19}\,\mathrm{cm}^{-3}$ were obtained but the incorporation of F drastically hindered the epitaxial growth of the ZnSe films. Consequently, only limited thicknesses of about 30 nm were achieved, then the growth regime changed to polycrystalline growth, which is unsuitable for our purpose. However, for Cl, successful epitaxial doping has already been reported.[2,3] Using similar growth conditions as in the latter references, we achieved Cl doping levels up to $2 \times 10^{19}\,\mathrm{cm}^{-3}$. We confirmed the doping concentration by SIMS and van der Pauw Hall measurements as depicted in Fig. S2 a. Both measurements are in good agreement although the free carrier concentrations extracted from Hall measure-

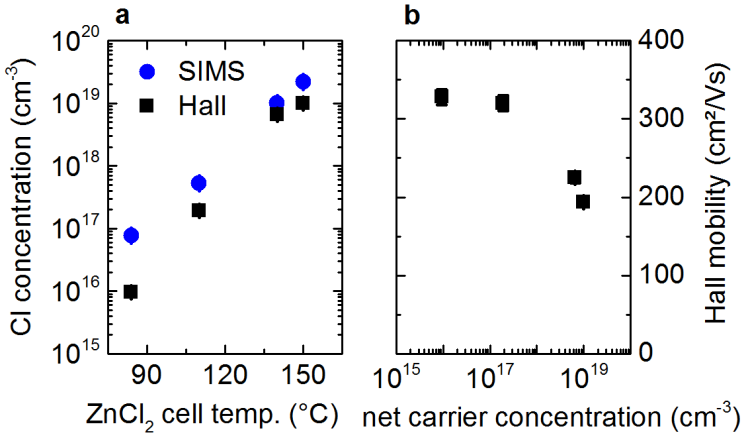

Figure S2: Characterization of ZnSe:Cl doped during MBE growth. a) Cl concentration versus $ZnCl_2$ cell temperature. Doping and carrier concentrations are investigated via SIMS analyses and van der Pauw measurements. b) Carrier mobility versus net charge carrier concentration determined by van der Pauw measurements.

ments are slightly lower than the quantified doping concentrations revealed by SIMS. This indicates that not all included Cl atoms are ionized and contribute to charge transport at RT.

Fig. S2 b shows the corresponding mobilities in ZnSe:Cl we derived from the Hall measurements as a function of the carrier concentration. Our dataset is in good agreement with typical literature values.[3,4] The observed reduction of the mobility for higher carrier concentrations is an expected trend as a higher amount of doping atoms leads to an increase of scattering centers. The prominent scattering mechanisms which limit the mobility in ZnSe:Cl are longitudinal optical phonon scattering at RT and impurity scattering at low temperature.[5]

Variation of contact metals and interface conditions

The optimization of the contact metal is performed on ZnSe:Cl samples which are doped *in-situ* during MBE growth. The figure of merit is the metal contact resistivity ρ_c. We use a Cl concentration of $n_{\mathrm{Cl}} > 1 \times 10^{19}\,\mathrm{cm}^{-3}$, which is on the metallic side of the MIT. According

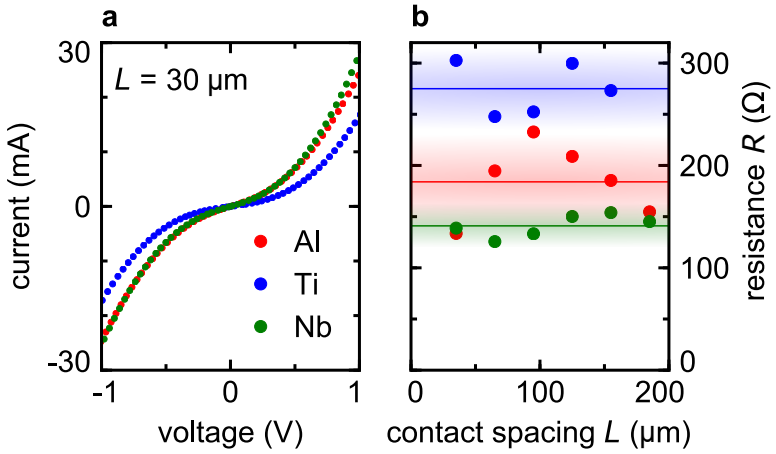

Figure S3: Metal contacts to highly doped ZnSe:Cl ($n_{\mathrm{Cl}} \approx 10^{19}\,\mathrm{cm}^{-3}$) fabricated by the *ex-situ* method. a) IV characteristics for three contact metals (Al, Ti, Nb) measured at RT. The distance between the contacts is $L = 30\,\mu\mathrm{m}$ for all three samples. b) Resistance R around zero bias as a function of the contact spaceing L as extracted from the IV curves for Al, Ti and Nb (same color code as in panel a). Horizontal lines and shaded areas indicate the mean resistance and variance, respectively.

to the Schottky model, a junction consisting of a metal and an n-type semiconductor exhibits ohmic IV characteristic for a low barrier height Φ_{bn0}[6]

$$\Phi_{\mathrm{bn0}} = q(\Phi_{\mathrm{m}} - \chi), \tag{1}$$

where q denotes the elementary charge, Φ_m the metal work function and χ the electron affinity of the semiconductor (χ=3.5 eV for ZnSe). The metals In, Mg, and Al providing a low work function Φ_{m} of 3.9 eV, 3.19 eV, and 4.13 eV, respectively, have been intensively experimentally studied in Ref. 7. Here, we study Ti, Al, and Mg together with Nb as another material with a low Φ_{m} of 4.0 eV.[8] For the *ex-situ* contacts the photoresist was inverted to a negative resist. The development was followed by metal deposition and a subsequent lift-off technique.

Fig. S3 a shows the IV characteristics of *ex-situ* fabricated contacts at a fixed contact distance $L = 30\,\mu\mathrm{m}$. The data was obtained by four-terminal measurements in darkness

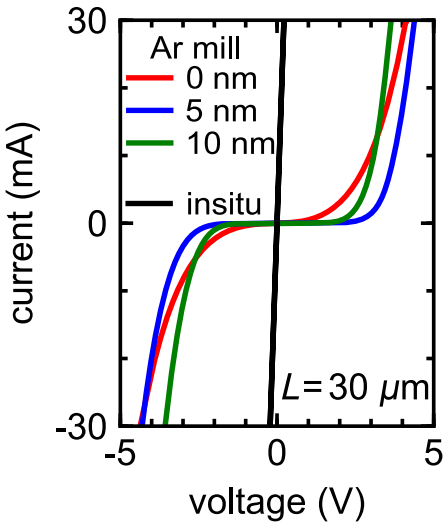

Figure S4: The effect of native oxide on ZnSe on the performance of Al contacts. The native oxide was removed by etching about 5 nm or 10 nm deep into the ZnSe surface via Ar milling. The corresponding IV characteristics (blue and green curves) indicate a substantial increase of the resistivity at low voltages compared to that of an untreated sample (red curve). The best ohmic contact performance is obtained with *in-situ* Al contacts (black curve).

at a needle probe station. The IV characteristics are non-linear for all metals and reveal a large resistance $R = 1/[\partial I/\partial V]_{V=0}$ around zero bias, which is the region of interest for qubit device operation. At elevated voltages, a higher current slope is observed and is symmetric for both electric field directions. The resistance R varies within one order of magnitude between samples and contacts and exhibits no monotonic dependence on the contact spacing (Fig. S3 b). Consequently, the device resistance is dominated by the contact resistance. We assume that a thin native oxide on ZnSe (presumably SeO) governs R as well as the breakdown characteristic at elevated voltages. Accordingly, the variation in R originates from nanoscale inhomogeneity of the junction. The lowest contact resistivities we obtained with the *ex-situ* method are of the order of $\rho_c \approx 10^{-2}\,\Omega\text{cm}^2$. This result is found for Nb and Al contacts while the contact resistance of Ti is substantially larger. Note that we assumed a homogeneous current density at the contact/semiconductor interface for extraction of the contact resistivity.

The ohmic contact performance of *ex-situ* samples is expected to be improved by oxide

removal in high vacuum and subsequent metal deposition. To realize this experimentally we utilize ion milling prior to Al metallization in the same vacuum chamber and afterwards a standard resist lift-off technique to form the contacts. For these experiments we used about 1 μm thick highly doped n-type ZnSe layers with a typical doping concentration of ($n_{\mathrm{Cl}} > 1 \times 10^{19}\,\mathrm{cm}^{-3}$). Neutral Ar ions impinging onto the substrate surface physically remove the oxide. The process is run in an Ar atmosphere of 1.6×10^{-4} mbar and Ar ions are pre-accelerated by a voltage of 80 mV before they are neutralized and hit the sample. With this process we determined typical etch rates of about 1 nm/s for ZnSe. For *ex-situ* Ar milled and *in-situ* samples the results of electrical characterization at room temperature are compared in Fig. S4. The IV curves obtained by four-terminal measurements in darkness are non-linear for all Ar ion milled samples. Thermionic transport limits electron transport across a barrier when the oxide is present. For the ion milled samples the total current can be increased at voltages of a few volt, but R is increased as well. We assume that crystal defects, namely Zn-vacancies, are introduced by the invasive etching process with Ar ions and decrease the net charge carrier concentration in the region where the contact is formed.[9] Lower carrier concentration leads to an effectively higher contact resistance and higher breakthrough voltages. In contrast, the *in-situ* contact provides linear IV characteristics at a significantly lower resistance level.

References

(1) Kim, Y. M.; Sleiter, D.; Sanaka, K.; Yamamoto, Y.; Meijer, J.; Lischka, K.; Pawlis, A. Semiconductor qubits based on fluorine implanted ZnMgSe/ZnSe quantum-well nanostructures. *Phys. Rev. B* **2012**, *85*, 085302.

(2) Karczewski, G.; Hu, B.; Yin, A.; Luo, H.; Furdyna, J. K. Deep electron states in chlorine-doped ZnSe films grown by molecular beam epitaxy. *Journal of Applied Physics* **1994**, *75*, 7382–7388.

(3) Ohkawa, K.; Mitsuyu, T.; Yamazaki, O. Characteristics of Cl-doped ZnSe layers grown by molecular-beam epitaxy. *Journal of Applied Physics* **1987**, *62*, 3216–3221.

(4) Miyajima, T.; Okuyama, H.; Akimoto, K. Ti / Pt / Au Ohmic Contacts to n-Type ZnSe. *Japanese Journal of Applied Physics* **1992**, *31*, 1743 – 1745.

(5) Jones, G.; Woods, J. The electrical properties of zinc selenide. *Journal of Physics D: Applied Physics* **1976**, *9*, 799–810.

(6) Sze, S. M. *Semiconductor Devices: Physics and Technology*; John Wiley & Sons Singapore Pte. Limited, 2012.

(7) Tyagi, M. S.; Arora, S. N. Metal zinc selenide schottky barriers. *Physica Status Solidi (a)* **1975**, *32*, 165–172.

(8) Trasatti, S. Work function, electronegativity, and electrochemical behaviour of metals: II. Potentials of zero charge and "electrochemical" work functions. *Journal of Electroanalytical Chemistry and Interfacial Electrochemistry* **1971**, *33*, 351–378.

(9) Laks, D. B.; Van de Walle, C. G.; Neumark, G. F.; Blöchl, P. E.; Pantelides, S. T. Native defects and self-compensation in ZnSe. *Physical Review B* **1992**, *45*, 10965–10978.